

## NEW PRECISION ORBITS OF BRIGHT DOUBLE-LINED SPECTROSCOPIC BINARIES. II. HR 2962, HD 214686, AND 16 PSC

JOCELYN TOMKIN<sup>1</sup> AND FRANCIS C. FEKEL<sup>2,3</sup>

<sup>1</sup> Astronomy Department and McDonald Observatory, University of Texas, Austin, TX 78712, USA; [jt@alexis.as.utexas.edu](mailto:jt@alexis.as.utexas.edu)

<sup>2</sup> Center of Excellence in Information Systems, Tennessee State University, 3500 John A. Merritt Boulevard, Box 9501, Nashville, TN 37209, USA; [fekel@evans.tsuniv.edu](mailto:fekel@evans.tsuniv.edu)

Received 2007 September 14; accepted 2007 November 11; published 2008 January 15

### ABSTRACT

Radial velocities from the 2.1 m telescope at McDonald Observatory and the coudé feed telescope at Kitt Peak National Observatory are used to determine new spectroscopic orbits for the double-lined spectroscopic binaries HR 2962 (F5V), HD 214686 (F8IV), and 16 Psc (F6Vb vw). The new orbital dimensions ( $a_1 \sin i$  and  $a_2 \sin i$ ) and minimum masses ( $m_1 \sin^3 i$  and  $m_2 \sin^3 i$ ) have accuracies of 0.1–1%. In the case of HD 214686, which has components of nearly the same mass ( $m_1/m_2 = 1.0080 \pm 0.0013$ ), we confirm that the component labeled as the primary in previous spectroscopic studies of this system is the slightly more massive component. We find that in HR 2962 the primary is rotating much more rapidly than the pseudosynchronous rate, while the rotation of the secondary is slightly faster than pseudosynchronous; in HD 214686 the primary is rotating at the pseudosynchronous rate or perhaps slightly less, while the rotation of the secondary is pseudosynchronous; and in 16 Psc both components rotate somewhat more rapidly than the pseudosynchronous rates. The three systems, which are of naked-eye brightness, are good potential targets for resolution by modern optical interferometers and so are promising candidates for full determination of their orbits and associated precise masses and distances.

*Key words:* binaries: spectroscopic

### 1. INTRODUCTION

If a binary is resolved as both a spectroscopic and visual binary, a full determination of its three-dimensional orbit is then possible. The spectroscopic orbit measures its linear size, while the visual orbit determines its orientation in space, and both types of orbit measure its eccentricity. Not only is the full orbit determined, but also the masses of the component stars and the distance to, or “orbital parallax” of, the system are fixed. Thanks mainly to advances in ground-based optical and near-infrared interferometry, the last 25 years or so have seen an increasing number of long-known spectroscopic binaries interferometrically resolved as visual binaries with consequent full determinations of their orbits, component masses, and distances. See Quirrenbach (2001), for example, for a review of progress in optical and infrared interferometry and a listing of spectroscopic binaries which have been resolved interferometrically and had their full orbits measured. More recently, a few additional systems have had their three-dimensional orbits determined (e.g., Hummel et al. 2001; Boden et al. 2006) and their resulting individual and system parameters compared with evolutionary theory.

In our series of papers, we report the determination of revised spectroscopic orbits for bright field spectroscopic binaries. The systems are of naked-eye, or near-naked-eye, brightness and are thus accessible to interferometry. The primary benefit of the program is the provision of new spectroscopic orbits that are a great improvement over those currently available in the literature, which mainly date from the photographic era of astronomy, and will complement prospective future interferometric observations. For some systems that hitherto

have been known only as single-lined spectroscopic binaries, an additional benefit is the detection of the secondary spectrum and measurement of secondary radial velocities for the first time. Our program uses new, high-resolution, red-wavelength spectra obtained with the 2.1 m telescope at McDonald Observatory and the coudé feed telescope at Kitt Peak National Observatory (KPNO)—see Fekel & Tomkin (2004) and Tomkin & Fekel (2006) for further details.

Our initial paper in this series (Tomkin & Fekel 2006) provided orbits for three systems: RR Lyn, 12 Boo, and HR 6169. Here we report new elements for three spectroscopic binaries with eccentric orbits: HR 2962, HD 214686, and 16 Psc. Table 1 gives basic data for the systems. All three are already known as double-lined spectroscopic binaries; in HR 2962 and 16 Psc the strengths of the primary and secondary lines are not greatly different, while in HD 214686 they are very similar. The most recent spectroscopic orbit determinations in the literature are by Harper (1926) for HR 2962, Bond et al. (1978) for HD 214686, and Cayrel de Strobel et al. (1974) for 16 Psc. We now look at the background of each system individually.

#### 1.1. HR 2962

This system has a combined spectral type of F5 V (Abt & Morrell 1995), an orbital period of 31.5 days, and a moderately eccentric orbit ( $e = 0.21$ ). Harper (1926) discovered the spectroscopic binary nature of the system and made the first and, to date, only determination of its orbit, which was based on radial velocities from 25 blue photographic spectrograms obtained at the Cassegrain focus of the 1.8 m telescope at the Dominion Astrophysical Observatory.

#### 1.2. HD 214686

This system has a spectral type of G0 in the Henry Draper Catalogue, and a more recent type of F8 IV (Harlan 1974), while Bond et al. (1978) used photometry on the *uvby* system

<sup>3</sup> Visiting Astronomer, Kitt Peak National Observatory, National Optical Astronomy Observatory, operated by the Association of Universities for Research in Astronomy, Inc. under cooperative agreement with the National Science Foundation.

**Table 1**  
Basic Properties of the Program Stars

Name	HR	HD	Spectral Type	$V^a$	$B - V^a$	Parallax <sup>a</sup> (mas)	Period (days)	Eccentricity
...	2962	61859	F5V	6.05	0.469	18.31	31.5	0.19
...	...	214686	F8IV	6.89	0.513	19.49	21.7	0.41
16 Psc	8954	221950	F6Vb vw	5.68	0.449	32.27	45.5	0.38

**Note.** <sup>a</sup> Perryman et al. (1997).

to infer an MK spectral type of F7 V for both stars in the system. The orbital period is 21.7 days, and the orbit is quite eccentric ( $e = 0.41$ ). The system is notable for the similarity of its spectra and near-equality of its masses. Sanford (1931) announced HD 214686 as a binary and made the first determination of its orbit, which used 61 blue photographic spectrograms obtained with the 100 in and 60 in reflectors at Mount Wilson Observatory in the years 1927–1930. As a result of the low resolution of these spectrograms (dispersion  $37 \text{ \AA mm}^{-1}$ ) and the eccentricity of the orbit, the primary and secondary lines were resolved on only 20 of these spectrograms, and these were limited entirely to the periastron branches of the velocity curves.

Bond et al. (1978) have redetermined the orbit. They reported two sets of radial velocities; a first set based on 22 spectrograms of  $6.6 \text{ \AA mm}^{-1}$  obtained at the Lick observatory 3 m coudé between 1970 and 1976 and a second smaller set based on observations made with four telescopes at four other observatories between 1972 and 1977. Rather than giving a solution of their combined velocities for the orbital elements, they chose to give separate solutions—one for each set of velocities. The two sets of elements are in good agreement, with the exception of  $K_2$ , which is distinctly smaller in the solution of the second set of velocities. We note that because  $K_1$  and  $K_2$  happen to be very similar, this means that in the solution of the Lick velocities  $K_2$  ( $= 55.9 \pm 0.35 \text{ km s}^{-1}$ ) is marginally larger than  $K_1$  ( $= 55.1 \pm 0.26 \text{ km s}^{-1}$ ), while in the solution of the velocities from the four other observatories  $K_2$  ( $= 51.6 \pm 0.7 \text{ km s}^{-1}$ ) is *smaller* than  $K_1$  ( $= 56.9 \pm 0.7 \text{ km s}^{-1}$ ); thus, in the first case the secondary is the less massive component, while in the second case it is the *more* massive component. Remarkably on this discrepancy, Bond et al. commented the Lick result “is probably to be preferred.” In the present study, because the Lick velocities are a majority of the Bond et al. velocities and because they are more accurate than the others, we will make use of them alone, and henceforth when we discuss the orbital elements determined by Bond et al., they will be those from their Lick velocities.

### 1.3. 16 Psc

This star has a combined spectral type of F6Vb vw (Barry 1970), an orbital period of 45.5 days, and an eccentric orbit ( $e = 0.37$ ). Its duplicity was discovered by Cayrel de Strobel (1968), who also made a preliminary determination of the orbit. Later Cayrel de Strobel et al. (1974) reported a thorough redetermination of the orbit, based on the 13 spectrograms used for the preliminary determination plus an additional 26 spectrograms, all of which were obtained with the coudé spectrographs of the 1.9 and 1.5 m telescopes at Haute Provence Observatory in the years 1967–1970. In commenting on their velocity curves and orbital solution, they remarked on possible systematic departures of the radial velocities of the secondary from its computed velocity curve and speculated that these non-Keplerian velocities might be signs of gaseous streams or a

gaseous ring associated with one or both components.

We also note the Thompson & Yeelin (2006) video recording of an occultation of 16 Psc by the asteroid 7 Iris on 2006 May 5 (UT date), which showed a stepped disappearance and reappearance and thus confirmed the duplicity of 16 Psc in a direct fashion quite independent of the knowledge long vouchsafed by spectroscopy.

## 2. OBSERVATIONS AND RADIAL VELOCITIES

Our observations were made at McDonald Observatory and KPNO from 2002 to 2007. The McDonald observations were acquired with the 2.1 m telescope, the Sandiford Cassegrain echelle spectrograph (McCarthy et al. 1993), and a Reticon CCD. The spectrograms cover the wavelength range 5700–7000  $\text{\AA}$  and have a resolving power of 49,000. The observations at KPNO were obtained with the coudé feed telescope, coudé spectrograph, and a TI CCD detector. All the spectrograms were centered at 6430  $\text{\AA}$ , cover a wavelength range of about 80  $\text{\AA}$ , and have a resolution of 0.21  $\text{\AA}$  or a resolving power of just over 30,000. Further details about the observations and data reduction are given in Tomkin & Fekel (2006).

The spectra of the three systems are double-lined and, at most orbital phases, the secondary lines are well separated from their primary counterparts. As already noted, in HD 214686 the primary and secondary line strengths are almost identical and in HR 2962 and 16 Psc they are not greatly different, thus in all three cases the primary and secondary stars are represented by numerous lines. The procedures used to measure the McDonald and KPNO radial velocities were described in our earlier paper. Here we content ourselves with recalling that the McDonald velocities are absolute velocities, which were set on a secure rest scale by means of the telluric  $\text{O}_2$  and  $\text{H}_2\text{O}$  lines embedded in the stellar spectra. The KPNO velocities were determined by cross-correlation with respect to IAU radial velocity standard stars of the same or similar spectral type as the program stars. The velocities adopted for those standards are from Scarfe et al. (1990). A comparison of the McDonald and KPNO velocities done in our earlier paper showed that they are consistent with each other to within 0.1–0.2  $\text{km s}^{-1}$  or better, so we decided, therefore, not to adjust either set of velocities, and we have likewise abstained from making any adjustment here. Table 2 gives the calendar dates, heliocentric Julian Dates, and heliocentric radial velocities for the McDonald and KPNO observations. Also given are the weights for the radial velocities categorized according to whether they are primary or secondary velocities and the telescope used.

## 3. DETERMINATION OF ORBITS AND RESULTS

### 3.1. HR 2962

Although our new radial velocities are much more precise than those of Harper (1926), the combination of the two provides

**Table 2**  
Radial Velocities of the Program Stars

Date (UT)	Tel	HJD -2,400,000	Phase	Velocity		Weight		O-C	
				Pri (km s <sup>-1</sup> )	Sec (km s <sup>-1</sup> )	Pri	Sec	Pri (km s <sup>-1</sup> )	Sec (km s <sup>-1</sup> )
HR 2962									
2002 Nov. 30	McD	52,608.925	0.8970	38.1	-71.6	0.05	1.00	-1.56	-0.13
2003 Mar. 21	McD	52,719.751	0.4153	-49.5	29.6	0.05	1.00	0.30	-0.02
2003 Apr. 21	McD	52,750.636	0.3958	-50.5	30.9	0.05	1.00	0.39	0.05
2004 Feb. 07	McD	53,042.891	0.6738	-9.2	-15.2	0.00	0.00	1.02	-0.10
2004 Feb. 09	McD	53,044.862	0.7363	3.1	-31.7	0.05	1.00	-1.85	0.54
2004 Apr. 13	McD	53,108.669	0.7620	13.3	-39.6	0.05	1.00	1.83	0.02
2004 Apr. 14	McD	53,109.679	0.7940	19.8	-49.0	0.05	1.00	0.19	-0.18
2004 Apr. 15	McD	53,110.666	0.8254	28.5	-57.4	0.05	1.00	1.33	-0.04
2004 Apr. 26	KPNO	53,121.624	0.1733	-30.6	8.2	0.05	1.00	0.41	-0.19
2004 Nov. 25	McD	53,334.921	0.9446	41.6	-72.5	0.05	1.00	1.10	-0.08
2004 Dec. 03	McD	53,342.954	0.1997	-36.9	15.6	0.05	1.00	0.56	-0.08
2005 Jan. 29	McD	53,399.882	0.0069	28.2	-59.3	0.05	1.00	-0.47	-0.24
2005 Jan. 30	McD	53,400.784	0.0355	19.0	-48.3	0.05	1.00	0.03	-0.21
2005 Jan. 31	McD	53,401.730	0.0656	6.9	-34.9	0.05	1.00	-0.38	-0.02
2005 Apr. 29	McD	53,489.618	0.8557	32.6	-64.5	0.05	1.00	-0.98	0.10
2005 May 02	KPNO	53,492.648	0.9519	40.3	-71.1	0.05	1.00	0.41	0.63
2005 Sep. 22	KPNO	53,636.024	0.5035	-40.8	19.2	0.05	1.00	0.37	-0.67
2005 Nov. 15	McD	53,689.932	0.2149	-38.7	19.5	0.05	1.00	1.89	0.29
2005 Nov. 16	McD	53,690.946	0.2471	-44.4	25.1	0.05	1.00	1.40	-0.01
2005 Nov. 17	McD	53,691.888	0.2770	-48.5	28.9	0.05	1.00	0.62	0.05
2006 Feb. 07	McD	53,773.834	0.8785	38.1	-69.1	0.05	1.00	0.68	-0.16
2006 Feb. 08	McD	53,774.824	0.9099	44.5	-72.6	0.05	1.00	3.85	-0.01
2006 Apr. 29	KPNO	53,854.649	0.4440	-47.3	27.4	0.05	1.00	0.33	0.24
2006 Apr. 30	KPNO	53,855.680	0.4768	-43.9	23.4	0.05	1.00	0.48	-0.10
2006 Nov. 07	McD	54,047.008	0.5507	-35.4	12.0	0.05	1.00	-1.06	-0.15
2007 Jan. 07	McD	54,107.869	0.4828	-42.3	22.6	0.05	1.00	1.40	-0.13
2007 Jan. 09	McD	54,109.898	0.5472	-33.6	12.6	0.05	1.00	1.29	-0.17
HD 214686									
2002 Oct. 20	McD	52,567.622	0.3882	-70.2	-2.7	1.00	1.00	-0.13	-0.12
2002 Dec. 02	McD	52,610.584	0.3679	-69.7	-2.9	1.00	1.00	0.09	-0.04
2003 Sep. 06	McD	52,888.806	0.1885	-51.5	-21.5	1.00	1.00	-0.09	-0.12
2003 Sep. 08	McD	52,890.778	0.2793	-65.2	-7.3	1.00	1.00	0.04	0.15
2004 Jun. 16	KPNO	53,172.973	0.2830	-65.2	-6.8	1.00	1.00	0.36	0.32
2004 Sep. 25	KPNO	53,273.751	0.9269	24.3	-97.8	1.00	1.00	-0.11	0.00
2004 Sep. 26	KPNO	53,274.745	0.9727	39.9	-113.2	1.00	1.00	0.13	0.08
2004 Sep. 27	KPNO	53,275.718	0.0176	31.8	-105.1	1.00	1.00	0.10	0.05
2004 Sep. 28	KPNO	53,276.757	0.0654	2.1	-75.3	1.00	1.00	-0.09	0.10
2004 Nov. 23	McD	53,332.608	0.6391	-56.9	-15.8	1.00	1.00	0.10	-0.05
2005 Jun. 11	KPNO	53,532.967	0.8717	-1.2	-72.1	1.00	1.00	-0.05	-0.06
2005 Sep. 21	KPNO	53,634.777	0.5632	-64.5	-8.7	1.00	1.00	-0.34	-0.16
2005 Oct. 20	McD	53,663.706	0.8962	9.8	-83.2	1.00	1.00	-0.10	-0.02
2005 Nov. 17	McD	53,691.672	0.1849	-50.6	-22.3	1.00	1.00	-0.03	-0.07
2006 Sep. 23	KPNO	54,001.812	0.4763	-68.7	-3.7	1.00	1.00	0.15	0.11
2006 Sep. 24	KPNO	54,002.804	0.5220	-66.8	-5.4	1.00	1.00	0.01	0.47
2006 Nov. 08	McD	54,047.645	0.5883	-62.2	-10.6	1.00	1.00	-0.07	-0.02
2006 Nov. 09	McD	54,048.615	0.6330	-57.8	-15.2	1.00	1.00	-0.10	-0.15
2006 Nov. 10	McD	54,049.579	0.6774	-52.2	-21.0	1.00	1.00	-0.17	-0.24
16 Psc									
2002 Oct. 19	McD	52,566.717	0.3453	35.1	63.9	0.50	1.00	0.06	-0.15
2002 Oct. 20	McD	52,567.659	0.3660	37.7	61.0	0.50	1.00	-0.13	-0.08
2002 Dec. 02	McD	52,610.610	0.3109	30.2	69.0	0.50	1.00	-0.08	-0.10
2003 Sep. 06	McD	52,888.840	0.4314	46.1	51.8	0.00	0.00	-0.18	-0.29
2003 Sep. 08	McD	52,890.818	0.4749	51.8	46.3	0.00	0.00	0.15	-0.08
2004 Sep. 11	McD	53,259.853	0.5930	65.2	31.6	0.50	1.00	-0.20	-0.15
2004 Sep. 12	McD	53,260.847	0.6148	67.8	29.2	0.50	1.00	-0.03	0.03
2004 Sep. 13	McD	53,261.838	0.6366	70.0	26.6	0.50	1.00	-0.21	-0.05
2004 Sep. 25	KPNO	53,273.782	0.8994	80.7	15.1	1.00	0.50	-0.17	-0.21
2004 Sep. 26	KPNO	53,274.755	0.9208	75.7	20.6	1.00	0.50	-0.08	-0.12
2004 Sep. 27	KPNO	53,275.757	0.9428	67.9	29.5	1.00	0.50	-0.01	0.41
2004 Nov. 23	McD	53,332.640	0.1941	13.5	86.8	0.50	1.00	-0.09	-0.05
2004 Nov. 25	McD	53,334.630	0.2379	19.7	80.3	0.50	1.00	-0.11	0.07
2005 Jan. 30	McD	53,400.570	0.6885	75.5	21.1	0.50	1.00	-0.14	0.23

**Table 2**  
(Continued)

Date (UT)	Tel	HJD −2,400,000	Phase	Velocity		Weight		O−C	
				Pri (km s <sup>−1</sup> )	Sec (km s <sup>−1</sup> )	Pri	Sec	Pri (km s <sup>−1</sup> )	Sec (km s <sup>−1</sup> )
2005 Jan. 31	McD	53,401.558	0.7102	78.0	18.6	0.50	1.00	0.22	0.00
2005 Sep. 21	KPNO	53,634.826	0.8417	85.8	10.4	1.00	0.50	0.04	0.29
2005 Sep. 22	KPNO	53,635.839	0.8639	85.2	11.2	1.00	0.50	0.17	0.32
2005 Nov. 15	McD	53,689.615	0.0469	14.8	86.2	0.50	1.00	0.70	−0.11
2005 Nov. 16	McD	53,690.666	0.0700	8.5	92.6	0.50	1.00	0.15	0.17
2005 Nov. 17	McD	53,691.690	0.0926	6.1	95.1	0.50	1.00	0.20	0.07
2006 Sep. 23	KPNO	54,001.838	0.9152	77.5	18.7	1.00	0.50	0.17	−0.38
2006 Sep. 28	KPNO	54,006.785	0.0240	23.5	76.1	1.00	0.50	0.00	−0.21
2006 Nov. 08	McD	54,047.672	0.9235	75.1	21.2	0.50	1.00	0.13	−0.39
2006 Nov. 09	McD	54,048.660	0.9452	67.4	30.1	0.50	1.00	0.52	−0.08
2007 Jan. 06	McD	54,106.565	0.2190	16.7	83.1	0.50	1.00	−0.39	−0.04
2007 Jan. 08	McD	54,108.549	0.2627	23.1	76.6	0.50	1.00	−0.30	0.18
2007 Jun. 14	KPNO	54,265.992	0.7261	79.3	16.9	1.00	0.50	0.03	−0.11
2007 Jun. 15	KPNO	54,266.976	0.7477	81.0	15.0	1.00	0.50	−0.18	0.02
2007 Jun. 16	KPNO	54,267.968	0.7696	82.8	13.2	1.00	0.50	−0.09	0.04
2007 Jun. 18	KPNO	54,269.983	0.8139	85.3	10.9	1.00	0.50	−0.06	0.37

**Table 3**  
Orbital Elements of HR 2962

Parameter	Harper (1926)	This Study <sup>a</sup>
<i>P</i> (days)	31.50	31.49978 (fixed)
<i>T</i> (HJD)	2,423,884.45 ± 0.33	2,453,399.66 ± 0.05
<i>e</i>	0.208 ± 0.045	0.1948 ± 0.0015
<i>ω</i> (deg)	44.0 ± 4.0	39.1 ± 0.5
<i>K</i> <sub>1</sub> (km s <sup>−1</sup> )	45.18 ± 1.94	46.60 ± 0.31
<i>K</i> <sub>2</sub> (km s <sup>−1</sup> )	52.43 ± 2.49	52.65 ± 0.07
<i>γ</i> (km s <sup>−1</sup> )	−12.11 ± 0.42	−12.51 ± 0.05
<i>m</i> <sub>1</sub> sin <sup>3</sup> <i>i</i> ( <i>M</i> <sub>⊙</sub> )	1.53	1.601 ± 0.010
<i>m</i> <sub>2</sub> sin <sup>3</sup> <i>i</i> ( <i>M</i> <sub>⊙</sub> )	1.32	1.417 ± 0.017
<i>a</i> <sub>1</sub> sin <i>i</i> (10 <sup>6</sup> km)	19.142	19.80 ± 0.13
<i>a</i> <sub>2</sub> sin <i>i</i> (10 <sup>6</sup> km)	22.214	22.370 ± 0.031
rms residual (km s <sup>−1</sup> ) (unit weight)	...	0.28

**Note.** <sup>a</sup> Solution of the new radial velocities alone with the period fixed at the value determined from a solution of the new radial velocities and those of Harper (1926) combined.

a much longer time base than ours alone, so we decided to make initial solutions of our velocities alone and our and Harper’s velocities combined. These showed that our velocities alone give more accurate results for all orbital elements, except for the period, which is better determined in the combined solution. We therefore adopted a solution of the new velocities alone with the period fixed at the value ( $P = 31.49978 \pm 0.00026$  days) determined from the initial combined solution. Table 3 gives the resulting orbital elements and, for comparison, those of Harper (1926), and Figure 1 shows the new primary and secondary velocities and the calculated velocity curves. It will be seen that the primary, which has somewhat broadened lines, has a slightly ragged velocity curve, while the secondary, which has narrow lines, has an extremely crisp one. Inspection of Table 3 shows that our new orbital elements are much more precise than Harper’s and, within the errors, are entirely consistent with his.

3.2. HD 214686

We have already reviewed the earlier determinations of the spectroscopic orbit of this system by Sanford (1931) and Bond et al. (1978). Although the combination of Sanford’s, Bond

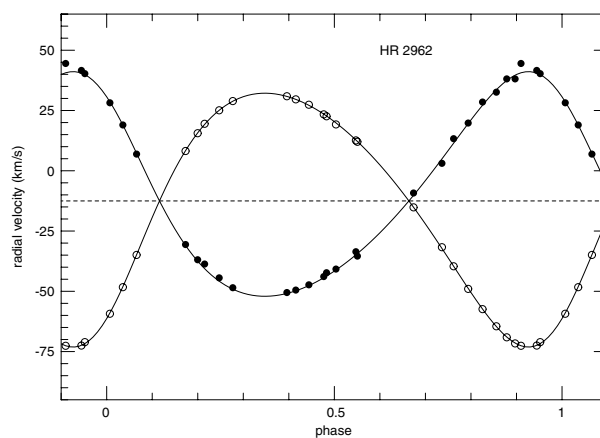


**Figure 1.** Radial velocities of HR 2962 compared with the computed velocity curves. Filled and open circles represent the primary and secondary, respectively. The primary, with its significantly broader lines, has the larger residuals to its computed curve.

et al.’s, and our velocities would provide the longest time base, it would only be about twice as long as the ~35 year time base

**Table 4**  
Orbital Elements of HD 214686

Parameter	Lick <sup>a</sup>	McD+KPNO+Lick <sup>b</sup>
$P$ (days)	$21.7014 \pm 0.0004$	$21.70116 \pm 0.00004$
$T$ (HJD)	$2,442,381.40 \pm 0.03$	$2,453,275.337 \pm 0.004$
$e$	$0.408 \pm 0.004$	$0.4071 \pm 0.0006$
$\omega$ (deg)	$17.4 \pm 0.6$	$16.32 \pm 0.10$
$K_1$ (km s <sup>-1</sup> )	$55.1 \pm 0.26$	$55.27 \pm 0.05$
$K_2$ (km s <sup>-1</sup> )	$55.9 \pm 0.35$	$55.71 \pm 0.05$
$\gamma$ (km s <sup>-1</sup> )	$-36.3 \pm 0.2$	$-36.456 \pm 0.024$
$m_1 \sin^3 i$ ( $M_\odot$ )	$1.18 \pm 0.024$	$1.178 \pm 0.0025$
$m_2 \sin^3 i$ ( $M_\odot$ )	$1.16 \pm 0.022$	$1.169 \pm 0.0025$
$a_1 \sin i$ ( $10^6$ km)	...	$15.066 \pm 0.015$
$a_2 \sin i$ ( $10^6$ km)	...	$15.184 \pm 0.015$
rms residual (km s <sup>-1</sup> ) (unit weight)	1.2	0.15

**Notes.**

<sup>a</sup> Solution of the Lick velocities of Bond et al. (1978).

<sup>b</sup> Solution of the McDonald, KPNO, and Lick velocities combined.

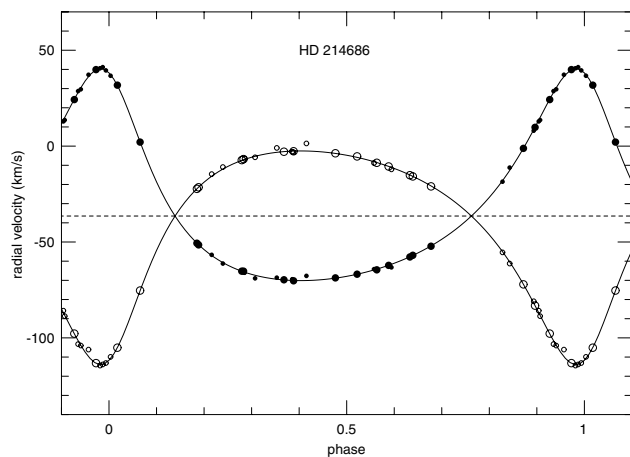


**Figure 2.** Radial velocities of HD 214686 compared with the computed velocity curves. Filled and open circles represent the primary and secondary, respectively. Larger circles are the new (McDonald and KPNO) velocities, while smaller circles are for the Lick velocities.

of Bond et al.'s and our velocities, while the quality of Sanford's velocities is much poorer than either Bond et al.'s or ours. We decided, therefore, to limit our attention to our new velocities and those of Bond et al. (And, as discussed earlier, we will use only the Lick velocities of Bond et al.)

Initial solutions of the new velocities alone and the new velocities combined with the Lick velocities showed that all orbital elements are better determined in the combined solution, with the improvement being most marked for the period determination. We adopted, therefore, this solution of the new and Lick velocities together as the final solution; its orbital elements are given in Table 4, and Figure 2 shows the primary and secondary velocities and the calculated velocity curves. Both velocity curves are very well defined and provide precise orbital elements. Inspection of Table 4 shows our new orbital elements and those for the Lick solution of Bond et al. are quite consistent. One also sees that  $K_1$  and  $K_2$  are extremely similar so that the mass ratio ( $m_1/m_2 = 1.0080 \pm 0.0013$ ) is very close to 1.0. Nonetheless it is sufficiently different from 1.0, considering the error, that we can be sure that the primary is the more massive component, as is expected for a binary composed of a pair of main-sequence stars.

Tokovinin et al. (2006) included HD 214686 in a sample

of 165 solar-type short-period binaries that were examined for additional components. They observed HD 214686 with an adaptive optics system but found no evidence of a third, more widely separated component. However, their note for this binary cryptically states "SB3?." Our orbital elements, determined from the combined set of velocities, are in excellent agreement with the previous solution of the Lick velocities alone (Bond et al. 1978) and thus, provide no spectroscopic evidence of a third component.

### 3.3. 16 Psc

As we have seen, Cayrel de Strobel et al. (1974) first determined this system's spectroscopic orbit using radial velocities from observations made at Haute Provence Observatory between 1967 and 1970. The first step, therefore, was to see if their velocities might usefully be combined with our new ones, and to this end we made preliminary solutions of the new velocities alone and the new and Haute Provence velocities combined. This showed the new velocities alone give better results for all orbital elements, with the exception of the period which is better determined in the combined solution. We therefore fixed the period at the value ( $P = 45.45850 \pm 0.00024$  days) from the combined solution and solved the new velocities alone for the other orbital elements. These new elements, along with the earlier ones of Cayrel de Strobel et al., are given in Table 5, and Figure 3 shows the primary and secondary velocities and the calculated velocity curves. Our new elements and those of Cayrel de Strobel et al. are quite consistent with each other, but we note that their value of  $(m_1 + m_2) \sin^3 i$  ( $= 3.49 M_\odot$ ) must be a gross overestimate; the actual value, implied by both their and our elements, is close to  $2.1 M_\odot$  (see Table 5 notes). The good agreement of the observed and calculated primary and secondary velocities, shown in Figure 3, leaves no room for the non-Keplerian effects in the secondary velocities reported by Cayrel de Strobel et al. and argues against the presence of gaseous streams or a gaseous ring.

## 4. SPECTRAL TYPES AND MAGNITUDE DIFFERENCE

Strassmeier & Fekel (1990) identified several luminosity-sensitive and temperature-sensitive line ratios in the 6430–6465 Å region. They employed those critical line ratios and the general appearance of the spectrum as spectral-type criteria. However, for stars that are hotter than early-G spectral class,

**Table 5**  
Orbital Elements of 16 Psc

Parameter	Cayrel de Strobel et al.	
	(1974) <sup>a</sup>	This Study <sup>b</sup>
$P$ (days)	$45.461 \pm 0.014$	45.45850 (fixed)
$T$ (HJD)	$2,439,777.367 \pm 0.295$	$2,453,323.815 \pm 0.021$
$e$	$0.370 \pm 0.015$	$0.3805 \pm 0.0006$
$\omega$ (deg)	$103.00 \pm 0.05$	$102.96 \pm 0.18$
$K_1$ (km s <sup>-1</sup> )	$40.10 \pm 0.53$	$40.11 \pm 0.05$
$K_2$ (km s <sup>-1</sup> )	$41.52 \pm 0.52$	$42.65 \pm 0.05$
$\gamma$ (km s <sup>-1</sup> )	$48.43 \pm 0.38$	$49.096 \pm 0.025$
$m_1 \sin^3 i$ ( $M_\odot$ )	... <sup>c</sup>	$1.090 \pm 0.004$
$m_2 \sin^3 i$ ( $M_\odot$ )	... <sup>c</sup>	$1.025 \pm 0.003$
$a_1 \sin i$ ( $10^6$ km)	23.29	$23.18 \pm 0.04$
$a_2 \sin i$ ( $10^6$ km)	24.11	$24.65 \pm 0.06$
rms residual (km s <sup>-1</sup> ) (unit weight)	...	0.17

**Notes.**

<sup>a</sup> Table 2, second iteration.

<sup>b</sup> Solution of the new radial velocities alone with the period fixed at the value determined from a solution of the new radial velocities and those of Cayrel de Strobel et al. (1974) combined.

<sup>c</sup> Cayrel de Strobel et al. give  $m_1/m_2$  and  $(m_1 + m_2) \sin^3 i$  instead of  $m_1 \sin^3 i$  and  $m_2 \sin^3 i$ . Their value of  $m_1/m_2$  ( $= 1.035$ ) is consistent both with their values of  $K_1$  and  $K_2$ , which give  $m_1/m_2 = 1.035 \pm 0.018$ , and ours, which give  $m_1/m_2 = 1.063 \pm 0.002$ . But their value of  $(m_1 + m_2) \sin^3 i$  ( $= 3.49 M_\odot$ ) must be in error because it is grossly inconsistent with both what their orbital elements imply ( $2.06 \pm 0.05$ ) and what we find ( $2.115 \pm 0.005$ ).

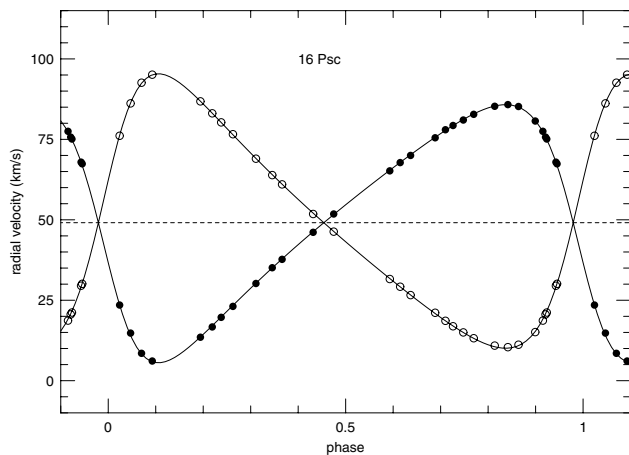


**Figure 3.** Radial velocities of 16 Psc compared with the computed velocity curves. Filled and open circles represent the primary and secondary, respectively.

the line ratios in that wavelength region have little sensitivity to luminosity. Thus, for the F stars of our three systems, we have used the entire 80 Å spectral region of our KPNO observations to estimate just the spectral classes of the individual components. The luminosity class may be determined by computing the absolute visual magnitude with the *Hipparcos* parallax and comparing that magnitude to evolutionary tracks or a table of canonical values for giants and dwarfs.

Spectra of our three binaries were compared with the spectra of a number of F-type stars primarily from the lists of Abt & Morrell (1995), Fekel (1997), and Gray (1989). The reference-star spectra were obtained at KPNO with the same telescope, spectrograph, and detector as our binary-star spectra. To facilitate a comparison, various combinations of the reference-star spectra were rotationally broadened, shifted in radial velocity, appropriately weighted, and added together with a computer program developed by Huenemoerder & Barden (1984) and

Barden (1985) in an attempt to reproduce the binary spectra.

The resulting best spectrum addition model is used to determine the continuum intensity ratio of the binary components at 6430 Å, a wavelength that is about 0.6 of the way between the central wavelengths of the Johnson *V* and *R* bandpasses. If the two stars have very similar spectral types, this intensity ratio is also the luminosity ratio and, thus, can be converted directly into a magnitude difference. However, if the lines of the secondary are intrinsically stronger than those of the primary, as would be the case, for example, if the components were main sequence stars of rather different spectral types, then the continuum intensity ratio results in a minimum magnitude difference.

#### 4.1. HR 2962

Spectral classifications of HR 2962 range from F2 V: by Bidelman (Abt & Bidelman 1969) to F6 III (Cowley 1976) and F7 Va (Barry 1970), while Cowley & Bidelman (1979) and Abt & Morrell (1995) both classified the combined spectrum as F5 V. Figure 4 is a spectrum of HR 2962 in the 6430 Å region and shows that although the line depths of the two components are similar, the line widths are quite different, with the primary having broad lines and the secondary having narrow lines. The reference star Procyon (F5 IV-V (Johnson & Morgan 1953) and mean  $[\text{Fe}/\text{H}] = -0.04$  (Taylor 2005)) produces excellent fits to the individual components. However, a simultaneous fit to both components results in a model spectrum with lines that are too weak. Thus, the system is apparently slightly metal rich compared to the Sun.

The continuum intensity ratio of the secondary/primary is 0.449. Given the similar spectral classes of the two components, we adopt this value as the luminosity ratio, which produces a magnitude difference of 0.87 with an estimated uncertainty of 0.1. This is also assumed to be the *V* magnitude difference. This difference and the *Hipparcos* parallax (Perryman et al. 1997) result in the absolute visual magnitudes determined in Section 5.1, which indicate that although the secondary

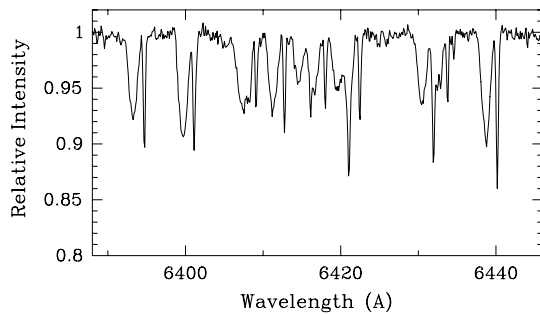


**Figure 4.** A portion of the 6430 Å region spectrum of HR 2962. The broad lines belong to the primary, the narrow lines, to the secondary. In this region iron lines dominate the spectrum.

is clearly a dwarf, the primary has begun to evolve significantly, and so we call it a subgiant. Thus, we classify the primary as an F5 subgiant and the secondary as an F5 dwarf.

#### 4.2. HD 214686

The only MK classification of HD 214686 is that of Harlan (1974), who found the combined system to be of type F8 IV. Bond et al. (1978) noted that the lines of the components are essentially identical, a result that our relatively high signal-to-noise spectra confirm. Thus, in our spectrum fits we used the same reference star for both components. We tried models with several stars that have spectral classes near F8 but slightly different iron abundances. Of those stars, the spectrum of HR 5694 (F8 IV-V (Johnson & Morgan 1953) and mean  $[\text{Fe}/\text{H}] = -0.09$  Taylor (2005)) provided an excellent fit to both components. The continuum intensity ratio of that fit is 0.961. Because the spectral classes of the two stars are identical, this value is also the luminosity ratio and produces a magnitude difference of  $0.04 \pm 0.05$  (estimated uncertainty), which we adopt as the  $V$  magnitude difference. We classify each star as an F8 dwarf, based on a comparison of its absolute visual magnitude, determined in Section 5.2, with the canonical values given by Gray (1992). The iron abundance of the best reference star suggests that the iron abundance of HD 214686 is slightly less than the solar value.

#### 4.3. 16 Psc

From Strömberg photometry results Cayrel de Strobel (1968) noted that 16 Psc is metal deficient, and soon afterward, Barry (1970) classified the composite system as F6 Vb vw, where the latter two letters indicate a star with very weak metal lines. Gray (1989) similarly found an F6 V spectral type and also specifically noted that 16 Psc is significantly metal deficient. On the other hand, Harlan (1974) and Abt & Morrell (1995) produced classifications that were three or four subclasses earlier, apparently accounting for the metal deficiency by assigning the system an earlier spectral class. The indications that 16 Psc is a metal-weak system provided a general starting point for our determination.

Although the more massive primary star has the slightly stronger and broader lines, the lines of the two components are generally similar, and so we have used the same comparison star for each component. Although we have a more limited selection of metal poor reference stars, we were able to compare the components of 16 Psc with HR 3262 (F6 V (Cowley 1976) and mean  $[\text{Fe}/\text{H}] = -0.31$  (Taylor 2005)) and with HR 4657

(F7 V m-2 (Gray 1989) and mean  $[\text{Fe}/\text{H}] = -0.7$  (Taylor 2005)). The former reference star spectrum can be adjusted to fit the individual components rather well, but a simultaneous fit to both components produces lines that are too strong. A fit to both components of 16 Psc with the more metal poor reference star results in lines that are too weak. To examine the possibility that a star with solar abundances but earlier spectral type might be appropriate, we also compared the spectrum of 16 Psc with that of HR 5075 (F2 V (Abt & Morrell 1995) and  $[\text{Fe}/\text{H}] = -0.04$  (Boesgaard & Tripicco 1986)). While many of the lines had approximately the right depths, some important line ratios are not correct. From these various comparisons, we estimate a spectral class of F6/7 for each component and conclude that the system is indeed metal poor with  $[\text{Fe}/\text{H}] \sim -0.5$ .

The continuum intensity ratio of the secondary/primary is 0.802. Given the similarity of the two components, we adopt this value as the luminosity ratio, which produces a magnitude difference of 0.24 with an estimated uncertainty of 0.1. This is also assumed to be the  $V$  magnitude difference. This difference and the *Hipparcos* parallax (Perryman et al. 1997) result in the absolute visual magnitudes determined in Section 5.3, which indicate that both components are dwarfs.

## 5. CIRCULARIZATION AND SYNCHRONIZATION

The two main theories of orbital circularization and rotational synchronization (e.g., Zahn 1977; Tassoul & Tassoul 1992) disagree significantly on absolute timescales but do agree that synchronization should occur first. The three systems discussed here have orbital periods between 21.7 and 41.5 days and eccentric rather than circular orbits. Duquennoy & Mayor (1991) examined the multiplicity of solar-type stars in the solar neighborhood. They found that while systems with periods  $\leq 10$  days had circular orbits, longer period orbits are generally eccentric. Thus, it is not surprising that our three systems have orbits with moderate eccentricities.

Hut (1981) has shown that in an eccentric orbit a star's rotational angular velocity will tend to synchronize with that of the orbital motion at periastron, a condition called pseudosynchronous rotation. With Equation (42) of Hut (1981), we calculated pseudosynchronous periods for the three systems.

Determining whether a component is pseudosynchronously rotating requires a measurement of its rotational velocity. We have obtained projected rotational velocities from our red-wavelength KPNO spectra with the procedure of Fekel (1997). His results for  $v \sin i$  values near  $5 \text{ km s}^{-1}$  (Table 1, Fekel 1997) are in good agreement with those of other groups. The unknown rotational inclination is generally assumed to be equal to the orbital inclination. The latter has been estimated by comparing our minimum masses with the expected mass for a given spectral type, tabulated in Table B1 of Gray (1992).

#### 5.1. HR 2962

To determine if the components of HR 2962 are pseudosynchronously rotating, we must first estimate their radii. Since the system is not a known eclipsing binary, we obtain the radii from the Stefan-Boltzmann law. From the *Hipparcos* catalog (Perryman et al. 1997) the  $V$  magnitude and  $B - V$  color of the HR 2962 system are 6.05 and 0.469, respectively. The *Hipparcos* parallax of  $18.31 \pm 0.095 \text{ mas}$  (Perryman et al. 1997) corresponds to a distance of  $55 \pm 3 \text{ pc}$ , and so we have assumed no interstellar reddening. As a result, the parallax, the  $V$  magnitude, and the adopted  $V$  magnitude difference of 0.87

(Section 4.1) were combined to obtain absolute magnitudes  $M_V = 2.76 \pm 0.12$  mag and  $M_V = 3.63 \pm 0.12$  mag for the primary and secondary, respectively. Because the components are nearly identical in spectral class, we adopted the observed  $B - V$  color of 0.469 (Perryman et al. 1997) for both components and then used Table 3 of Flower (1996) to obtain the bolometric corrections and effective temperatures of the two components. With adopted effective temperatures of 6,413 K and estimated uncertainties of 150 K for the two stars, the resulting luminosities of the primary and secondary are  $L_1 = 6.2 \pm 0.7 L_\odot$  and  $L_2 = 2.8 \pm 0.3 L_\odot$ , respectively, while the radii are  $R_1 = 2.03 \pm 0.15 R_\odot$  and  $R_2 = 1.36 \pm 0.10 R_\odot$ , respectively. The uncertainties in the computed quantities are dominated by the parallax uncertainty plus, to a lesser extent, the effective temperature uncertainty.

The orbit of HR 2962 has a modest eccentricity of 0.195, which results in a pseudosynchronous period of 25.6 days. Combining the pseudosynchronous period and the above radii, we obtain pseudosynchronous rotational velocities of 4.0 and 2.7 km s<sup>-1</sup> for the primary and secondary, respectively. For HR 2962 our  $v \sin i$  values, averaged from four spectra, are  $38.3 \pm 2.0$  and  $4.9 \pm 1.0$  km s<sup>-1</sup> for the primary and secondary, respectively.

The minimum masses of the two components are relatively large, indicating that the orbital inclination is not too far from 90°. Indeed, the minimum mass of the F5 dwarf secondary is greater than its expected value (Gray 1992). However, the 31.5 day orbital period makes the possibility of eclipses unlikely. Adopting a somewhat smaller inclination of 80° does not significantly increase our projected rotational velocities. Given the uncertainty in our  $v \sin i$  value for the secondary, that component may be rotating slightly faster than pseudosynchronous, while the primary is clearly rotating much more rapidly. The canonical masses for various spectral types (Gray 1992) suggest that the primary likely began its main sequence life as a late-A-type star.

### 5.2. HD 214686

Similar to HR 2962, the answer to the question of whether the components of HD 214686 are pseudosynchronously rotating begins with estimates of the components' radii. From the *Hipparcos* catalog (Perryman et al. 1997) the  $V$  magnitude and  $B - V$  color of the HD 214686 system are 6.89 and 0.513, respectively. The *Hipparcos* parallax of  $19.49 \pm 1.19$  mas (Perryman et al. 1997) corresponds to a distance of  $51 \pm 3$  pc, and so we have assumed no interstellar reddening. As a result, the parallax, the  $V$  magnitude, and the adopted  $V$  magnitude difference of 0.04 (Section 4.2) were combined to obtain absolute magnitudes  $M_V = 4.07 \pm 0.13$  mag and  $M_V = 4.11 \pm 0.13$  mag for the primary and secondary, respectively. Because the components are nearly identical, we adopted the observed  $B - V$  color of 0.513 (Perryman et al. 1997) for both components and then used Table 3 of Flower (1996) to obtain the bolometric corrections and effective temperatures of the two components. With adopted effective temperatures of 6,227 K and estimated uncertainties of 100 K for the two stars, the resulting luminosities of the primary and secondary are  $L_1 = 1.9 \pm 0.2 L_\odot$  and  $L_2 = 1.8 \pm 0.2 L_\odot$ , respectively, while the radii are  $R_1 = 1.19 \pm 0.08 R_\odot$  and  $R_2 = 1.17 \pm 0.08 R_\odot$ , respectively. The uncertainties in the computed quantities are dominated by the parallax uncertainty plus, to a lesser extent, the effective temperature uncertainty.

Because the orbit of HD 214686 has a moderately large ec-

centricity of 0.407, the pseudosynchronous period of 10.39 days is less than half of the orbital period. Combining the pseudosynchronous period and the above radii, we obtain pseudosynchronous rotational velocities of 5.8 and 5.7 km s<sup>-1</sup> for the primary and secondary, respectively. For HD 214686 our  $v \sin i$  values, averaged from ten spectra, are  $4.3 \pm 1.0$  and  $5.1 \pm 1.0$  km s<sup>-1</sup> for the primary and secondary, respectively. While the estimated uncertainties result in overlapping  $v \sin i$  values, in every spectrum measured the primary's lines were narrower than the secondary's, and therefore, we believe that the primary really does have the smaller projected rotational velocity. The minimum masses of the components are close to the canonical value for F8 dwarfs (Gray 1992), and so they suggest that the orbital inclination is not far from 90°. Bond et al. (1978) provided ephemerides for possible eclipses, and from our orbital elements we find that eclipses require an orbital inclination  $\geq 87^\circ$ . From the limited amount of *Hipparcos* photometry, the *Hipparcos* team gave the variability type of HD 214686 as constant (Perryman et al. 1997), so there was no obvious evidence of eclipses in their data. For comparison purposes we adopt a somewhat smaller, but still rather high, inclination of 80°. This value for the orbital inclination and the assumption that the rotational inclination has the same value, produces equatorial velocities of 4.4 and 5.2 km s<sup>-1</sup>. Thus, the estimated rotational velocities are similar to the pseudosynchronous velocities, with the primary rotating perhaps slightly slower than its pseudosynchronous velocity, while the secondary may be rotating pseudosynchronously.

### 5.3. 16 Psc

To see if the components of 16 Psc are pseudosynchronously rotating, we once again need to estimate the radii of the components. From the *Hipparcos* catalog (Perryman et al. 1997) the  $V$  magnitude and  $B - V$  color of the 16 Psc system are 5.69 and 0.449, respectively. The *Hipparcos* parallax of  $32.27 \pm 0.84$  mas (Perryman et al. 1997) corresponds to a distance of  $31.0 \pm 0.8$  pc, and so we have assumed no interstellar reddening. As a result, the parallax, the  $V$  magnitude, and the adopted  $V$  magnitude difference of 0.24 (Section 4.3) were combined to obtain absolute magnitudes  $M_V = 3.86 \pm 0.06$  mag and  $M_V = 4.10 \pm 0.06$  mag for the primary and secondary, respectively. Because the components are nearly identical, we initially adopted the observed  $B - V$  color of 0.449 (Perryman et al. 1997) for both components. However,  $B - V$  is affected by metallicity (e.g., Gray 1994), and so we corrected for this effect with Gray's Equation (3), which produces  $B - V = 0.51$ . We then used this corrected color and Table 3 of Flower (1996) to obtain the bolometric corrections and effective temperatures of the two components. With adopted effective temperatures of 6,239 K and estimated uncertainties of 150 K for the two stars, the resulting luminosities of the primary and secondary are  $L_1 = 2.3 \pm 0.1 L_\odot$  and  $L_2 = 1.8 \pm 0.1 L_\odot$ , respectively, while the radii are  $R_1 = 1.30 \pm 0.07 R_\odot$  and  $R_2 = 1.16 \pm 0.07 R_\odot$ , respectively. The uncertainties in the computed quantities are dominated by the parallax uncertainty plus, to a lesser extent, the effective temperature uncertainty.

Because the orbit of 16 Psc has a moderately large eccentricity of 0.380, the pseudosynchronous period of 23.55 days is nearly one-half that of the orbital period. Combining the pseudosynchronous period and the above radii, we obtain pseudosynchronous rotational velocities of 2.8 and 2.5 km s<sup>-1</sup> for the primary and secondary, respectively. For 16 Psc our  $v \sin i$  values, averaged from ten spectra, are  $9.5 \pm 1.0$  and

$6.3 \pm 1.0 \text{ km s}^{-1}$  for the primary and secondary, respectively. Thus, both components are clearly rotating more rapidly than the pseudosynchronous rates.

The minimum masses of both components are greater than  $1 M_{\odot}$ , suggesting a moderately high orbital and presumably similar rotational inclination. An orbital inclination of  $70^{\circ}$  results in masses of  $1.31$  and  $1.24 M_{\odot}$ , which correspond to spectral types F5 V and F7 V, respectively (Gray 1992), in good agreement with the spectral type of the combined system.

## 6. SUMMARY

We have determined new and precise spectroscopic orbits for the bright double-lined spectroscopic binaries HR 2962, HD 214686, and 16 Psc. The linear sizes of the relative orbits ( $a \sin i$ ), which are  $(42.17 \pm 0.13) \times 10^6 \text{ km}$  (HR 2962),  $(30.250 \pm 0.021) \times 10^6 \text{ km}$  (HD 214686), and  $(47.83 \pm 0.07) \times 10^6 \text{ km}$  (16 Psc), combined with the distances (Table 1) lead to corresponding angular sizes of the apparent orbits of 5.2 mas for HR 2962, 3.9 mas for HD 214686, and 10.3 mas for 16 Psc. Angular separations of this sort are well within the scope of modern optical interferometers so when our spectroscopic results are complemented by prospective high-quality interferometric results accurate three-dimensional orbits, masses, and distances for the systems will follow. In the case of HD 214686, which has a mass ratio very close to 1.0 and for which there was some doubt as to which component is the more massive, we find that the primary is, indeed, the more massive component, as expected for a binary composed of two main-sequence stars. We find that the components of all three systems are rotating at pseudosynchronous rates or faster.

We thank David Doss for his patient guidance, which was essential for the successful operation of the 2.1 m telescope at McDonald and its instrumentation, and Daryl Willmarth for his support of the KPNO coudé feed observations. The research at Tennessee State University was supported in part by NASA grant NCC5-511 and NSF grant HRD-9706268.

## REFERENCES

- Abt, H. A., & Bidelman, W. P. 1969, *ApJ*, **158**, 1091  
 Abt, H. A., & Morrell, N. I. 1995, *ApJS*, **99**, 135  
 Barden, S. C. 1985, *ApJ*, **295**, 162  
 Barry, D. C. 1970, *ApJS*, **76**, 324  
 Boden, A. F., Torres, G., & Latham, D. W. 2006, *ApJ*, **644**, 1193  
 Boesgaard, A., & Tripicco, M. 1986, *ApJ*, **303**, 724  
 Bond, H. E., Walter, D. K., Wallerstein, G., Morbey, C. L., & Popper, D. M. 1978, *PASP*, **90**, 679  
 Cayrel de Strobel, G. 1968, *Astrophys. Lett.*, **1**, 173  
 Cayrel de Strobel, G., Fracassini, M., & Pasinetti, L. E. 1974, *A&A*, **37**, 179  
 Cowley, A. P. 1976, *PASP*, **88**, 95  
 Cowley, A. P., & Bidelman, W. P. 1979, *PASP*, **91**, 83  
 Duquenois, A., & Mayor, M. 1991, *A&A*, **248**, 485  
 Fekel, F. C. 1997, *PASP*, **109**, 514  
 Fekel, F. C., & Tomkin, J. 2004, *Astron. Nachr.*, **325**, 649  
 Flower, P. J. 1996, *ApJ*, **469**, 355  
 Gray, D. F. 1992, *The Observation and Analysis of Stellar Photospheres*, (Cambridge: Cambridge Univ. Press)  
 Gray, D. F. 1994, *PASP*, **106**, 1248  
 Gray, R. O. 1989, *AJ*, **98**, 1049  
 Harlan, E. A. 1974, *AJ*, **79**, 682  
 Harper, W. E. 1926, *Publ. Dom. Astrophys. Obs.*, **3**, 265  
 Huenemoerder, D. P., & Barden, S. C. 1984, *BAAS*, **16**, 510  
 Hummel, C. A., et al. 2001, *AJ*, **121**, 1623  
 Hut, P. 1981, *A&A*, **99**, 126  
 Johnson, H. L., & Morgan, W. W. 1953, *ApJ*, **117**, 313  
 McCarthy, J. A., Sandiford, B. A., Boyd, D., & Booth, J. 1993, *PASP*, **105**, 881  
 Perryman, M. A. C., et al. 1997, *A&A*, **323**, L49  
 Quirrenbach, A. 2001, *Ann. Rev. Astron. Astrophys.*, **39**, 353  
 Sanford, R. F. 1931, *ApJ*, **74**, 201  
 Scarfe, C. D., Batten, A. H., & Fletcher, J. M. 1990, *Publ. Dominion Astrophys. Obs.*, **18**, 21  
 Strassmeier, K. G., & Fekel, F. C. 1990, *A&A*, **230**, 389  
 Tassoul, J.-L., & Tassoul, M. 1992, *ApJ*, **395**, 259  
 Taylor, B. J. 2005, *ApJS*, **161**, 444  
 Thompson, B., & Yeelin, T. 2006, *PASP*, **118**, 1648  
 Tokovinin, A., Thomas, S., Sterzik, M., & Udry, S. 2006, *A&A*, **450**, 681  
 Tomkin, J., & Fekel, F. C. 2006, *AJ*, **131**, 2652  
 Zahn, J.-P. 1977, *A&A*, **57**, 383